15th World Congress on Computational Mechanics (WCCM-XV)
8th Asian Pacific Congress on Computational Mechanics (APCOM-VIII)
Virtual Congress: 31 July – 5 August 2022
S. Koshizuka (Ed.)

Consideration of the Behaviour of a Wind Turbine Wake Using High-Fidelity CFD Simulations

KOICHIRO SHIBUYA[1,2], TAKANORI UCHIDA[3], MASAKI INUI[1], ZHIREN BAI[4] AND YOSHIHIRO TANIYAMA[5]

[1]Engineering and Technology Development Department, Wind Power Business Unit, Carbon Neutral Solution Business Headquarters, Hitachi Zosen Corporation, 7-89, Nankokita 1-chome, Suminoe-ku, Osaka 559-8559, Japan,
shibuya.k@hitachizosen.co.jp (https://www.hitachizosen.co.jp)

[2]Dept. Mechanical and Systems Engineering, Kyushu University, 6-1 Kasuga-koen, Kasuga, Fukuoka 816-8580, Japan

[3]Research Institute for Applied Mechanics (RIAM), Kyushu University, 6-1 Kasuga-koen, Kasuga, Fukuoka 816-8580, Japan,
takanori@riam.kyushu-u.ac.jp

[4]Department of Mechanical Engineering, Osaka University, 2-1, Yamadaoka, Suita-shi, Osaka 565-0871, Japan,
haku@combu.mech.eng.osaka-u.ac.jp

[5]Mechanical Engineering R&D Department, Energy Systems Research and Development Center Toshiba Energy Systems & Solutions Corporation, 8, Shinsugita-Cho, Isogo-ku, Yokohama-shi, Kanagawa 235-8523, Japan,
yoshihiro.taniyama@toshiba.co.jp

Key words: Wind turbine wakes, Large-eddy simulation (LES), Actuator line model, Wind direction fluctuations

Abstract. *During operation of a wind turbine, wake flow occurs behind the wind turbine, reducing the amount of power generation and the life of the downwind wind turbine. To understand wind turbine wake flow, Computational Fluid Dynamics (CFD) simulations were conducted using "RIAM-COMPACT" to reproduce wind turbine wake flow. There is no significant difference in the flow field of the wind turbine wake between upwind-type and downwind-type turbines. In the 5D downstream of the wind turbine, the vertical distribution of the mainstream velocity component is almost the same regardless of the power of the inflow profile in the swept area. When the inflow wind has a wind direction change of up to 10 degrees, the wind turbine wake is quite diffuse, and its vertical distribution is in good agreement with the field measurements made by the vertical profile lidar.*

1 INTRODUCTION

In recent years, there has been a growing demand for the use of renewable energy due to concerns about extreme weather conditions caused by global warming, and the development stage of wind farms is transitioning from land to offshore where energy density is greater. In a wind farm, multiple wind turbines are located in one area to generate large amounts of power more efficiently. When wind turbines are installed offshore, they are arranged in a dense configuration with close proximity to each other to reduce the cost of power transmission lines. However, when the wind turbines are operating in the presence of wind, a region called a wake appears behind the turbines where the wind energy is lost, and the wind speed is reduced.

Figure 1 is a photograph of the Horns Rev wind farm in Denmark, showing the wakes behind the wind turbines visualized by fog[1].

Figure **2** shows a schematic illustration of a wake. The wakes form a highly turbulent flow field due to the complex interference of the swirling flow caused by the rotation of the wind turbine blades, the blade tip vortices ejected from the blade tips, and the detached vortices from the hub and tower. In Figure 1, another wind turbine can be seen in the wake visualized by the fog. Under these conditions, the downstream wind turbines not only generate less power, but also have a shorter life span due to turbulence[2]. In order to keep operating costs of wind farms low and to continue to generate large amounts of electricity, it is important to accurately understand wind turbine wakes.

We have conducted research on wind turbine wakes since 2018. In our efforts, the wakes characteristics of real wind turbines have been analyzed from wind tunnel experiments, Computational Fluid Dynamics (CFD) simulations, and real wind observations, and a new practical wakes model[3] has been developed that can be used for LES numerical fluid dynamics simulations. In this paper, some results of the joint research on wind turbine wakes are presented.

Figure 1: Wind turbine wake visualized by fog in Horns Rev Wind Farm[1]

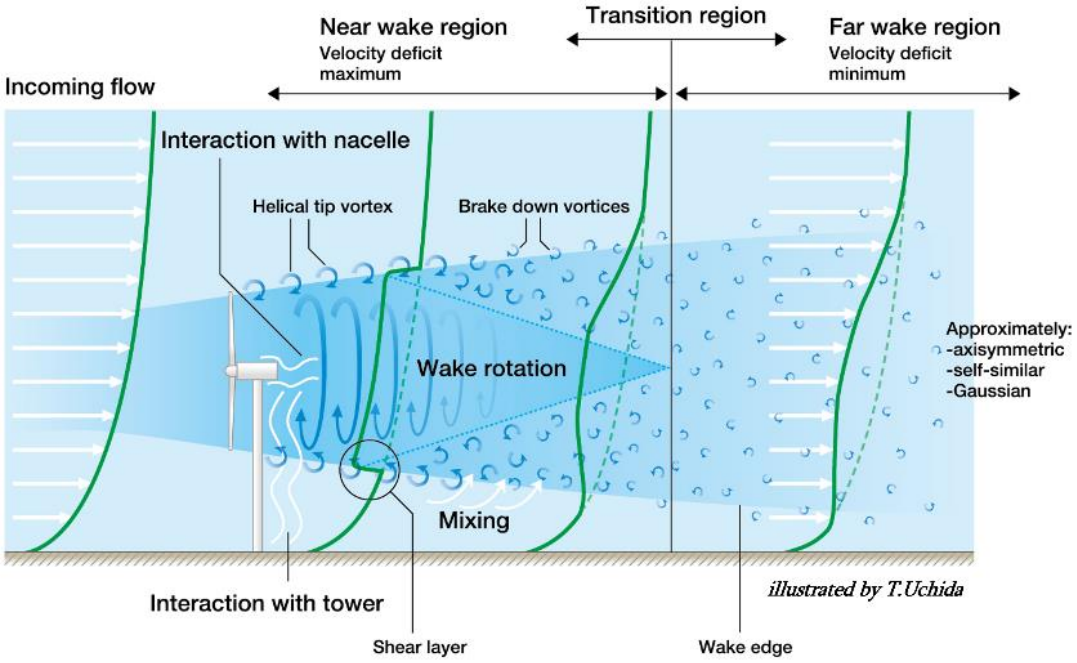

Figure 2: Schematic diagram of wind turbine wake configuration

2 CFD SIMULATIONS OF WIND TURBINE WAKES BY RIAM-COMPACT

2.1 Calculation conditions

Three-dimensional CFD simulations using a wind turbine model were conducted to understand the characteristics of wind wakes. The finite difference method was used, and Large-Eddy Simulation (LES) was employed as the turbulence model. For modeling the sub grid scale (SGS) component, a mixed time-scale model[4] was employed, which is computationally stable and does not require a wall damping function. Simpson's rule is applied for the explicit filter operation, and the coupling algorithm for the velocity and pressure fields is a partial step method based on the Euler explicit method[5]. The Poisson equation for the pressure was obtained by a relaxation calculation using the Successive Over-Relaxation (SOR) method. For the discretization of the spatial terms, the convection terms were obtained using a modified third-order upwind scheme based on the interpolation method with a fourth-order central difference and a numerical viscosity term for the fourth-order derivative. The weight of the numerical viscosity term in the third-order upwind scheme is 3.0 in the Kawamura-Kuwahara scheme[6], which is generally used, but in this study, it is set to 0.5 to keep its influence sufficiently small. The second-order central difference was applied to the other spatial terms.

The rotating wind turbine blades are modeled using the Actuator Line (AL) model[7], which is based on blade element theory. The flow field caused by the wind turbine can be expressed by adding the fluid force generated by the blade according to the wind speed and blade rotation speed to the external force term in the Navier-Stokes equation. In this calculation, the wind turbine blades were set to rotate at a peripheral speed ratio of 4.0, which maximizes the power

coefficient.

As shown in Figure 3, the dimensions of computational domain are 524m, 230m, and 186m in the *x*-, *y*-, and *z*-directions, respectively, and an orthogonal grid with a grid resolution of 0.43m is created. The total numbers of grid points are 1121, 341, and 329 points in the *x*, *y*, and *z* directions, respectively, for a total of approximately 120 million points.

Slip conditions were imposed on the upper and lateral boundaries, non-slip conditions on the ground, and convective outflow conditions on the outflow boundary. For nacelles and towers, velocities were set to zero for all grid points contained therein. The pressure boundary condition was set to the Neumann condition for all boundaries. The Reynolds number based on the blade diameter D and the inflow velocity U_{hub} at the hub height was set to Re ($=U_{hub}D/\nu$) $=2\times10^4$, and the dimensionless time step was set to $\Delta t=1\times10^{-3}$. In this calculation, time integration was performed for dimensionless times t=200-400.

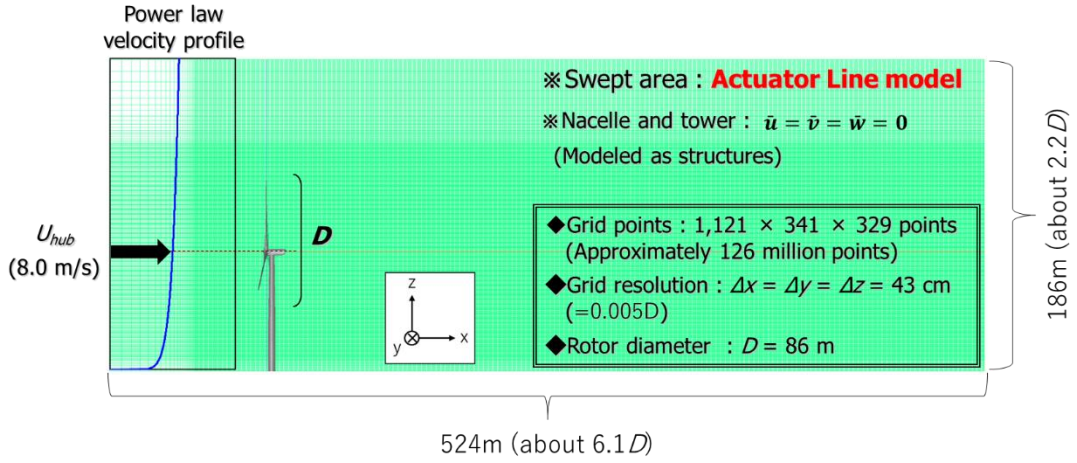

Figure 3: Computational grid in CFD simulation

2.2 Comparison of simulations with different wind turbine geometries and inflow wind profiles

In this paper, the wakes formed by upwind-type and downwind-type wind turbines are compared by simulation, and the effects of the wakes on incoming winds with different vertical profile shapes are also compared[8]. The details of the comparison are shown in Table 1. The upwind-type turbine has the wind-receiving surface upstream of the tower, while the downwind-type turbine has the surface downstream of the tower. It is known that the wind speed increases with height, and the following power law holds empirically.

$$v(z) = Az^{\frac{1}{N}} \tag{1}$$

where z is the height above ground, $v(z)$ is the wind speed at height z above ground, N is a power exponent, and A is a proportionality constant. Equation(1) can be rewritten using certain ground heights z_1 and z_2 as follows

$$v(z_2) = \left(\frac{z_2}{z_1}\right)^{\frac{1}{N}} v(z_1) \quad (2)$$

In this calculation, $v(z_1)$=U_{hub}=8m/s in equation(2) was set so that the wind speed at the hub height is 8m/s for all power exponential conditions.

Table 1: Comparison performed in the simulation

Comparison Case	Wind Turbine Type	Power Number (*N*)
Case A	Upwind	10
	Downwind	
Case B	Downwind	4
		10
		20

Figure 4 shows the contour of the velocity in the main flow direction (instantaneous field at dimensionless time *t*=10) for the results of comparison Case A. The wakes formed by the upwind-type and downwind-type turbines are not significantly different. No significant difference in the wakes formed by the upwind-type and downwind-type turbines was observed, and both figures show that the flow behind the turbines is turbulent and the wind speed is significantly reduced. The simulation also reproduces a blade tip vortex ejected from the blade, which disintegrates as it flows downstream. The separation flow from the tower and nacelle has an effect close to the wind turbine, but away from the turbine, the overall effect of the wake due to the blades dominates.

Figure 5 shows the results of the comparison Case B calculation. In Figure 5, it can be seen that the wind inflow in case (c) is closer to a uniform flow than in case (a). The wakes formed behind the wind turbine flowed along the inflow wind profile immediately after the formation.

Figure 6 shows the averaged vertical profiles of the calculated results 5*D* behind the wind turbine from the wind-receiving surface. Although there are differences in the overall profile depending on the power law, the profiles of the wind turbine receiving surface are consistent in all cases, indicating that similar wakes are formed behind the wind turbine regardless of the geometry of the wind turbine and the shape of the incoming wind.

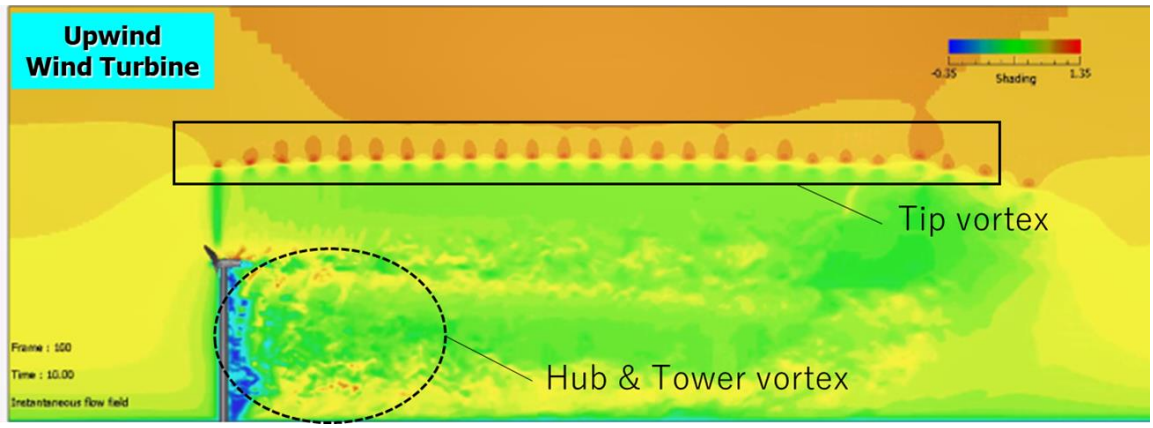

(a)

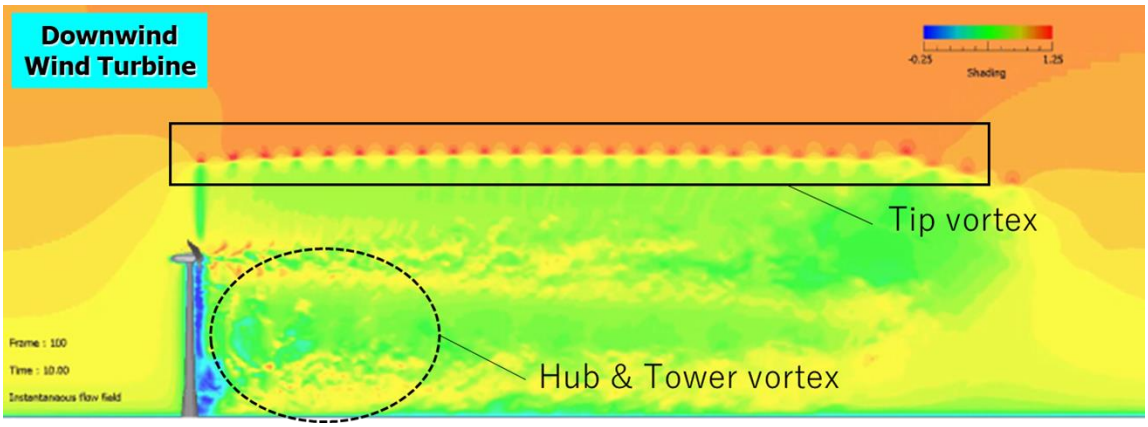

(b)

Figure 4: Comparison of wakes formed by different wind turbine types (at dimensionless time t=10): (a) upwind type, (b) downwind type

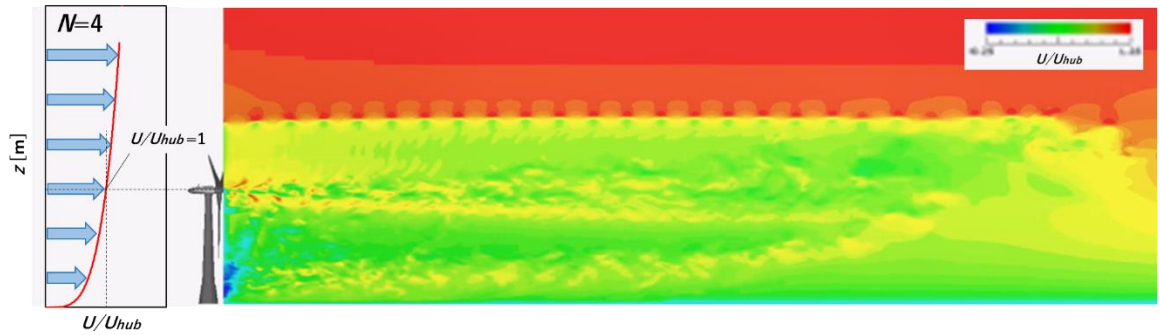

(a)

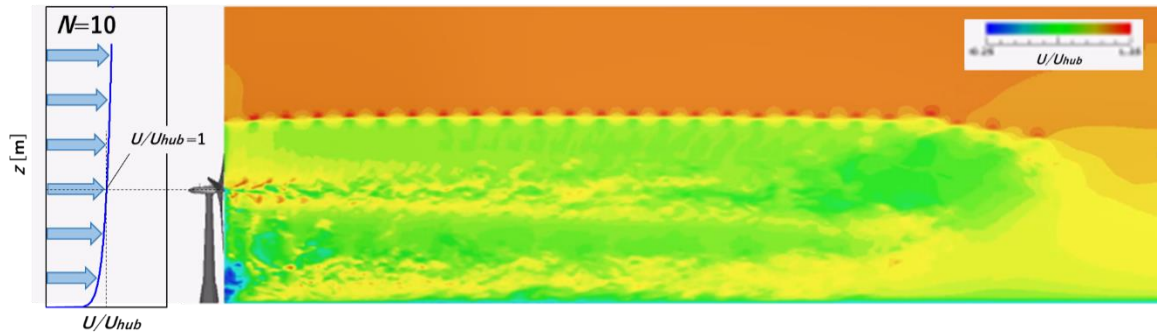

(b)

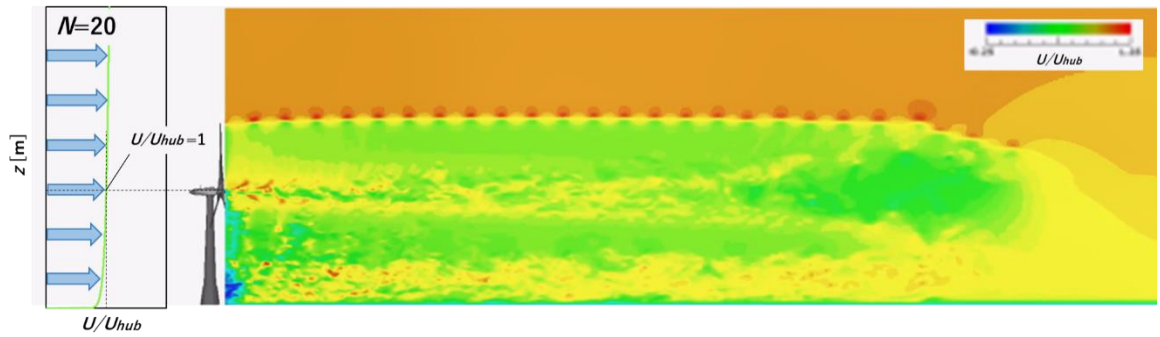

(c)

Figure 5: Comparison of wind turbine wakes formed under different inflow wind profile shapes (at dimensionless time t=10): power number is (a) N=4, (b) N=10, (c) N=20

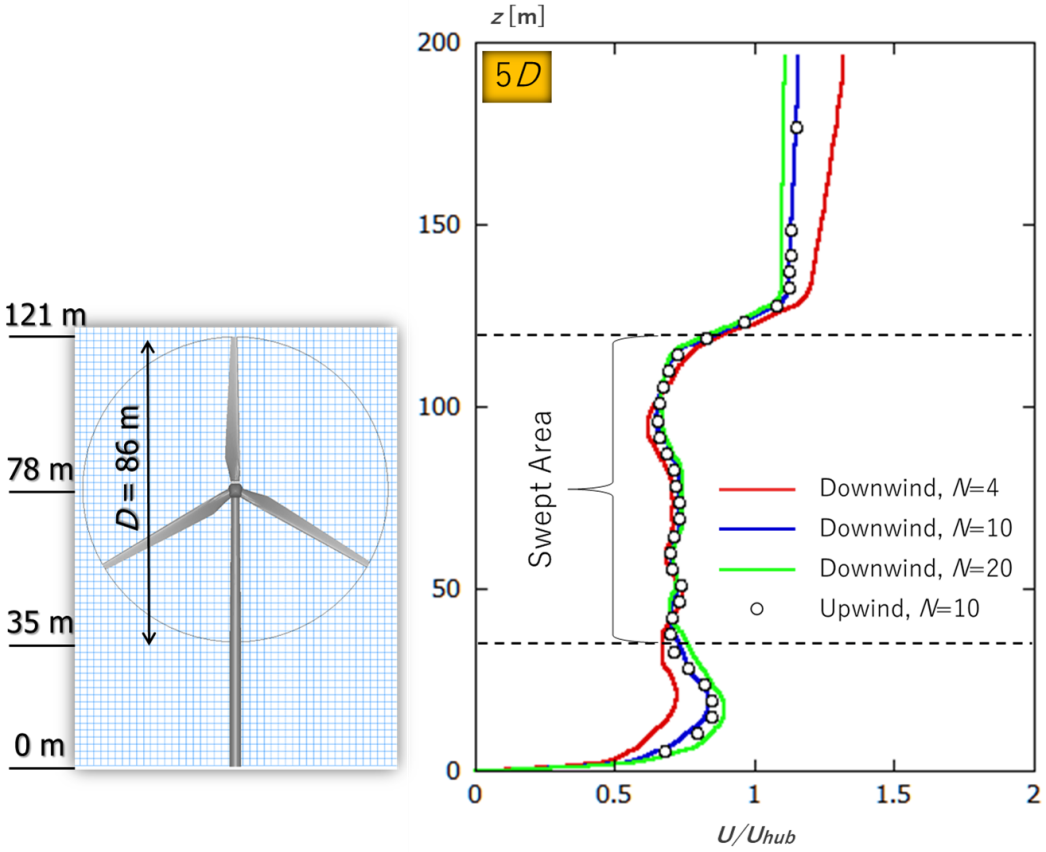

Figure 6: Comparison of vertical profiles of wake velocity for each condition

3 SIMULATIONS TAKING INTO ACCOUNT VARIATIONS IN WIND DIRECTION

3.1 A wind turbine wake formed in real wind conditions

In wind tunnel experiments and CFD simulations, it is assumed that the wind is blowing straight ahead, but in actual wind conditions, the wind direction changes constantly, so it is necessary to take this effect into account in practical studies. We analyzed Supervisory Control And Data Acquisition (SCADA) data of two wind turbines at the Omonogawa Wind Power Plant in Akita prefecture, Japan, shown in

Figure 7, and evaluated the wake of the No. 2 wind turbine, which affects the No. 1 turbine.

Figure 8 shows the relationship between the standard deviation of wind direction (defined as wind direction variation in this paper) and the rate of wind speed deficit due to wakes. The wind direction variation has a significant effect on the velocity deficit, which affects the power generation evaluation. We simulated the behavior of wind turbine wakes under wind direction variation using the computational solver described above.

	Item	Value
No.2	Model	HTW2.0-86
	Rated Power	2 MW
	Rotor Diameter (D)	86 m
	Hub height from sea level	82 m

	Item	Value
No.1	Model	HTW2.0-80
	Rated Power	2 MW
	Rotor Diameter	80 m
	Hub height from sea level	89 m

Figure 7: Omonogawa Wind Farm in Akita Prefecture, Japan

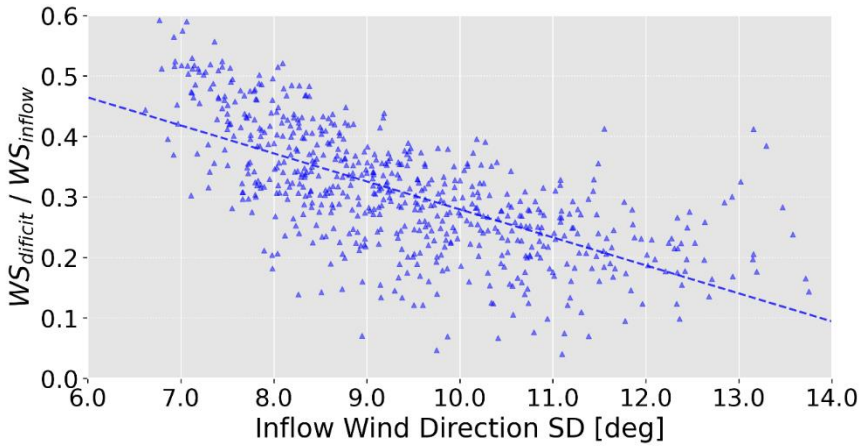

Figure 8: Correlation between standard deviation of wind direction and velocity deficit of a wind turbine wake

3.2 Simulation with continuously varying wind direction

In order to perform wake simulations under variable wind direction, calculations were performed by continuously changing the wind direction flowing into the computational domain[9].

Figure 9 shows a schematic diagram of the time-varying wind direction with a maximum angle of 10 degrees. As shown in the figure, the wind direction was set to change at a constant angle with time. The angle of wind direction change per calculation step is set at 2.5×10^{-4}

degrees to avoid oscillations in the solution due to sudden changes in the flow field. In this calculation, time integration was performed over a dimensionless time period t=0~320.

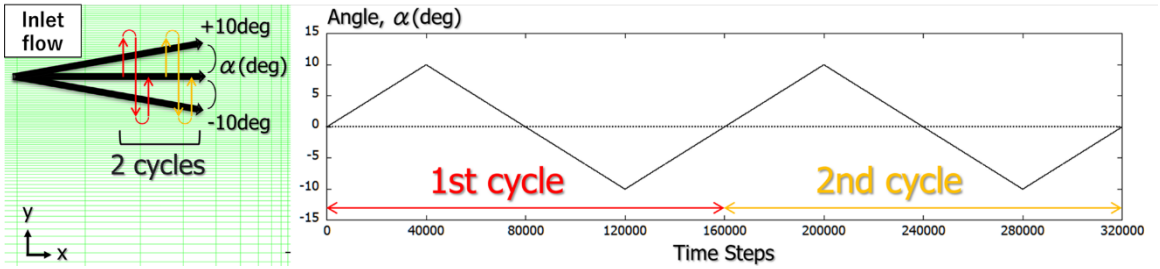

Figure 9: Schematic view of the continuously changing wind direction

Figure 10 compares the simulation results with a vertical lidar of the wind speed of a wind turbine behind 3*D*. For more information on the vertical lidar observation method, please refer to the literature[10]. The simulation results agree well with the measurement results when the wind direction variation is set to a maximum of 10 degrees. The simulation results deviated significantly from the observed data when the wind direction was fixed, as in wind tunnels and general CFD simulations, and it can be said that simulations that take wind direction fluctuations into account are important for understanding the wakes of actual wind turbines.エラー! 参照元が見つかりません。 shows a contour plot of the wind velocity at the hub height (center of rotation height) of the wind turbine. Pattern (a) shows the inflow pattern with a fixed wind direction, and pattern (b) shows the inflow pattern with a 10-degree wind direction variation. When the wind direction is variable, the wakes are spread to the left and right, which means that in a wind farm, not only the wind turbines directly behind but also many of those downwind of the wind turbines are affected by the wakes.

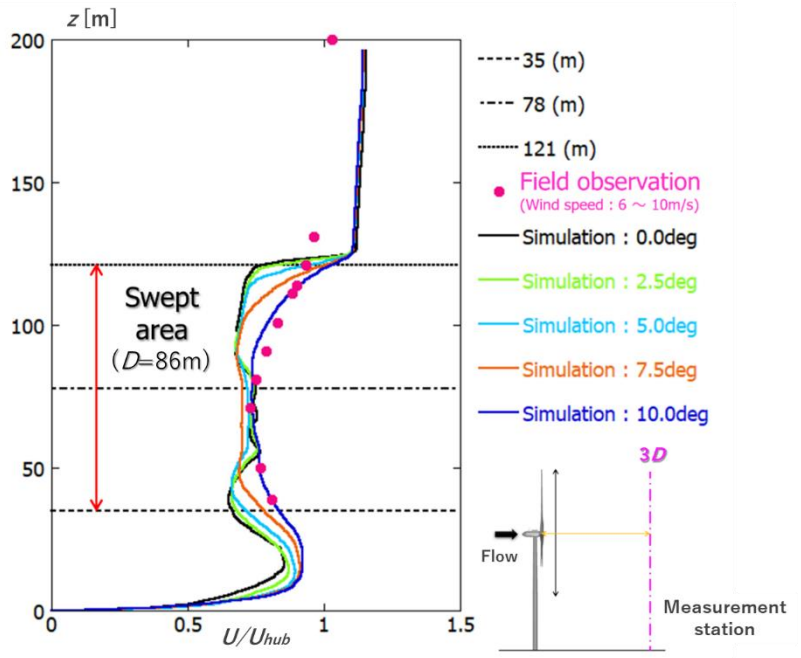

Figure 10: Comparison of vertical profiles of wind turbine wake velocity under variable inflow wind direction conditions

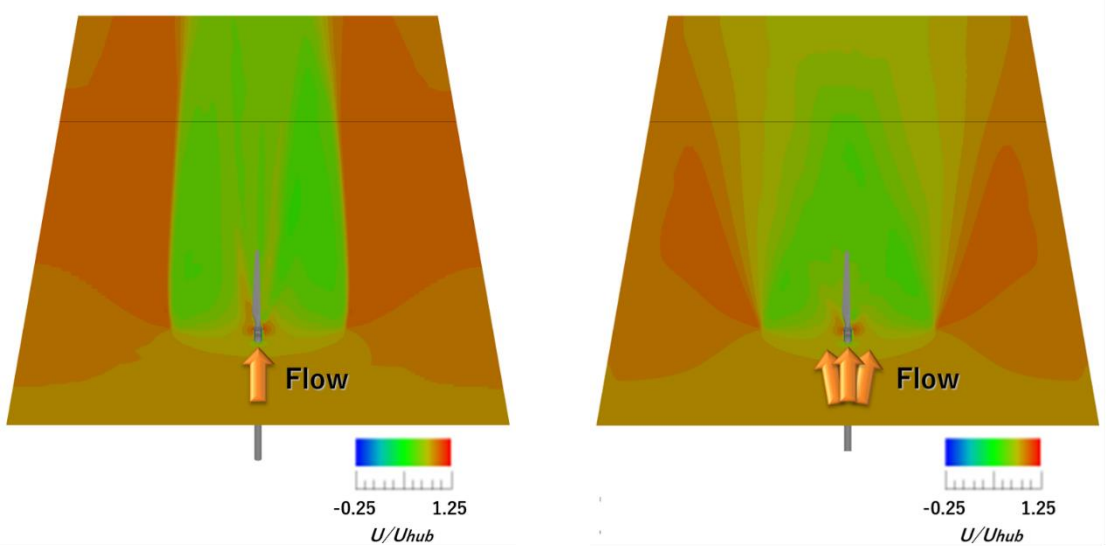

(a) (b)

Figure 11: Comparison of average flow field of a wind turbine wake under variable inflow wind direction conditions (in the horizontal plane): (a) fixed inlet wind direction, (b) continuously changing inlet wind direction

4 CONCLUSIONS

CFD simulations using LES were performed to understand the flow behind a wind turbine, and the following findings were obtained.

- The flow field behind the wind turbine is not significantly different between the upwind-type and downwind-type wind turbines.
- At position 5*D* downstream of the wind turbine, the vertical profile of the main flow velocity component is almost the same regardless of the shape of the inflow profile.
- When the inflow wind has a maximum value of 10 degrees wind direction variation, the wake of the wind turbine is considerably diffuse, and the results of its vertical profile agree well with the results of the field measurements by the vertical profile lidar.

REFERENCES

[1] Hasager, C. B., Nygaard, N. G., Volker, P. J. H., Karagali, I., Andersen, S. J. and Badger, J. Wind Farm Wake: The 2016 Horns Rev Photo Case. Energies **2017**, *10*, 317.

[2] Thomsen, K., Sørensen, P. Fatigue loads for wind turbines operating in wakes. J. Wind Eng. Ind. Aerodyn. **1999**, *80*, 121-136.

[3] Uchida, T., Taniyama, Y., Fukatani, Y., Nakano, M., Bai, Z.R., Yoshida, T. and Inui, M. A New Wind Turbine CFD Modeling Method Based on a Porous Disk Approach for Practical Wind Farm Design. Energies **2020**, *13*, 3197.

[4] Inagaki, M., Kondoh, T. and Nagano, Y. A mixed-time-scale SGS model with fixed model-parameters for practical LES. ASME. J. Fluids Eng. **2005**, *127*, 1–13.

[5] Kim, J. and Moin, P. Application of a fractional-step method to incompressible Navier-Stokes equations. J. Comput. Phys. **1985**, *59*, 308.

[6] Kawamura, T., Takami, H. and Kuwahara, K. Computation of high Reynolds number flow around a circular cylinder with surface roughness. Fluid Dyn. Res. **1986**, *1*, 145–162.

[7] Sørensen, J. N. and Shen, W. Z. Numerical modeling of wind turbine wakes. JOURNAL OF FLUIDS ENGINEERING-TRANSACTIONS OF THE ASME **2002**, *124*, 393-399.

[8] Uchida, T. Effects of Inflow Shear on Wake Characteristics of Wind-Turbines over Flat Terrain. Energies, **2020**, *13*, 3745.

[9] Uchida, T. and Gagnon, Y. Effects of continuously changing inlet wind direction on near-to-far wake characteristics behind wind turbines over flat terrain. J. Wind Eng. Ind. Aerodyn, **2022**, *220*, 104869.

[10] Uchida, T., Yoshida, T., Inui, M. and Taniyama, Y. Doppler Lidar Investigations of Wind Turbine Near-Wakes and LES modeling with New Porous Disc Approach. Energies **2021**, *14*, 2101.